

Daria KOSTKA^{1,2,*}, Agnieszka GOGLER-PIGŁOWSKA², Wiktoria PŁONKA¹,
Damian SOJKA², Małgorzata ADAMIEC-ORGANIŚCIOK²,
Magdalena SKONIECZNA¹, Dorota ŚCIEGLIŃSKA^{2,*}

Chapter 3. A TOOL FOR QUANTIFYING THE LEVEL OF ANTIGEN (KERATIN 10) DETERMINED BY THE IHC METHOD IN HUMAN EPIDERMAL EQUIVALENTS OBTAINED IN VITRO

3.1. Introduction

The 3D organotypic co-culture system is an up-to-date culture technique that enables generation of the reconstructed human epidermis (RHE) in vitro. This culture system is considered superior to standard two-dimensional in vitro culture of keratinocytes in plastic dishes. Keratinocytes when grown in air-liquid interface in 3D co-culture with dermal equivalent form complex tissue that replicates the dermal-epithelial crosstalk, polarized protein distribution and architectural features characteristic of each cell layer seen in normal human epidermis in vivo. Despite some drawbacks (lack of immune system cells and melanocytes), the application of RHE model have enabled to address previously inaccessible questions on human keratinocyte differentiation and epidermal regeneration. Furthermore 3D organotypic co-culture method is very powerful when combined with methods of genetic manipulations of keratinocytes such as genes knockout (deletion), knockdown (downregulation) or knockin (insertion). Such a combination provides a strong platform for investigating how the integrity, structure and functions of human epidermis are connected to protein function.

¹ Department of Systems Biology and Engineering and Biotechnology Centre, Silesian University of Technology, Gliwice, Poland.

* Corresponding author: darikos556@student.polsl.pl

² Center for Translational Research and Molecular Biology of Cancer, Maria Skłodowska-Curie National Research Institute of Oncology Gliwice Branch, 44-102 Gliwice, Poland.

* Corresponding author: dorota.scieglinska@io.gliwice.pl

One of the steps in the algorithm for evaluation of genetically modified keratinocytes in RHE model is the detection of keratinocyte differentiation markers. This task is performed to gain knowledge on how a particular genetic modification made in cells effects on their potential to differentiate and generate full-length RHE. Alterations in differentiation marker(s) location or changes in their expression levels in RHE model usually represent changes in epithelial stratification and reflect aberrant keratinocyte differentiation. Analysis of differentiation markers expression is routinely executed using immunohistochemistry (IHC) method in order to detect some of marker proteins that are specific for an early, moderate or late keratinocyte differentiation stages. However quantitative analysis of the IHC results in RHE samples can be a challenging task. One of the available IHC staining analysis programs is Fiji with the Immunohistochemistry (IHC) Image Analysis Toolbox. This program was designed for the analysis of images, where the specimen covers the entire photo area. In case of RHE, the specimen occupies a small part of the image. This fact may have significant effect on results as the background signal might bias the IHC staining signal quantitation. Therefore, this study was undertaken to address abovementioned issue and develop a tool that could be used to quantify results of IHC detection of antigens in RHE samples.

3.1.1. The structure and functions of the skin and the epidermis

The skin is the most external and one of the largest human organs. Human skin is composed of three layers: epidermis, dermis and subcutaneous tissue. It consists of glands, hair, nails, blood vessels, lymphatic and nerve endings [1]. The function of the skin is to protect the inside of the body against the influence of the environment, physical and chemical damages, infections, UV radiation [1, 2]. This organ is also required to maintain a stable condition of the internal body environment, protect against dehydration and regulate body temperature [3].

The epidermis, a type of stratified squamous keratinizing epithelium, constitutes the outermost layer of the skin. It is composed mainly of keratinocytes organized in hierarchical manner. Stem cells building the top of hierarchy are located in the basal layer, their progeny differentiate along with moving towards the epidermal surface. During epidermal differentiation keratinocytes' morphology transits from large cells with large nuclei of the basal layer through polygonal cells with large multi-lobed

nuclei of the spinous layer into spindle-shaped flattened cells of the granular layer and ultimately into enucleated spindle-shaped corneocytes of the stratum corneum [1, 4]. Corneocytes are dead cells filled with keratin fibers embedded in the filaggrin matrix. These cells are built into lipid matrix that form the extracellular shell termed the corneocyte envelope. The lipid coat on the cells' surface is the essential component of the epidermal permeability barrier that protects the body from excessive water loss and absorption of exogenous substances [1, 4].

Epidermal differentiation is a cycle of transformation that lasts from 26 to 42 days. During homeostasis, keratinocytes differentiate from basal proliferating cells to nuclear-depleted squamous corneocytes. The process of keratinocytes differentiation requires the activation of the genes that are implicated in functional and structural cell transformation. Genes related to the differentiation process are concentrated in the Epidermal Differentiation Complex (EDC) [2, 5, 6].

The characteristic components of the epidermis are keratins, a fibrillar protein that builds intermediate filaments. Some of them are considered as differentiation markers in the epidermal keratinocytes. Keratin 10 (K10) represents an early differentiation marker that is expressed in keratinocytes located in the spinous layer. As keratinocytes leave the basal layer and pass to the spinous layer, they inhibit the production of keratin 5 and keratin 14, and activate the production of keratin 1 (K1) and K10. The expression of K1 and K10 is activated under the conditions of the increasing Ca^{2+} concentration [7]. These structural proteins are crucial for proper function and structure of epidermis. For example removal of the K10 gene in mouse model resulted in skin fragility similar to that of patients suffering from epidermolytic hyperkeratosis [8]. The keratinocytes in the upper spinous layer also produce another differentiation markers such as involucrin, a component of the corneocyte envelope, and transglutaminase K, an enzyme that catalyzes a critical step in the formation of the cornified envelope of terminal differentiation [9, 10, 11].

3.1.2. Immunohistochemical reactions

Immunohistochemistry (IHC) is a standard technique that employs antibodies to detect and quantify a specific protein (antigen) within a given tissue. The method is designed in a way that allows microscopic observation of the antigen-antibody complexes. The antigen is specifically recognized by a primary antibody. The detection of a primary

antibody-antigen complex in an IHC experiment can be either direct or indirect. Direct detection methods employ primary antibody directly conjugated to a label (dye or enzyme) [12]. Indirect reactions employ additional usage of a secondary antibody that is labelled and directed against the host species of the primary antibody (unlabeled). Indirect reactions are usually used to increase signal (staining) intensity [12].

The color effects in IHC are frequently generated using antibody (primary or secondary) labelled with an enzyme such as the horse radish peroxidase (HRP). Addition of a specific substrate (i.e. a chromogen) gives a colored product. One of the most popular chromogens is 3,3-diaminobenzidine tetrahydrochloride called DAB. To act as a dye, DAB is oxidised and converted to an insoluble polymer, which precipitates as a dark brown pigment at the reaction site allowing visualization of the target molecule [13, 14].

3.1.3. The role of Heat Shock Protein A2 (HSPA2) in the epidermis

HSPA2 belongs to the multigene *HSPA* (*HSP70*) family of chaperone proteins playing important roles in the maintenance of cellular proteostasis. HSPA2 was initially described as a testis-specific protein, which is crucial for spermatogenesis and male fertility [15]. However, as we showed previously, HSPA2 is also present in selected human somatic tissues including stratified and pseudostratified epithelia. In the epidermis HSPA2 accumulates in basal keratinocytes [16]. The role of HSPA2 in the epidermis and also in other epithelia is poorly understood.

In our preliminary study we showed that HSPA2 can regulate keratinocyte differentiation. We observed that decrease in the HSPA2 protein levels in keratinocytes, resulting from partial inhibition of the *HSPA2* gene expression by the RNAi mechanism, resulted in a more differentiated but still proliferative cell phenotype [17]. In order to examine the effect of a total lack of HSPA2 on keratinocyte differentiation we generated CRISPR/Cas9-mediated knockout of the *HSPA2* gene expression in immortalized human epidermal keratinocyte HaCaT line. Histological and IHC evaluation showed altered stratification of RHE generated from HSPA2-null cells. Among other altered pattern of immunostaining with approved differentiation markers such as K10 and others occurred in HSPA2-null RHE. Therefore, semiquantitative analysis of differentiation markers expression would help to

describe in more details how a lack of HSPA2 impairs epidermis stratification in RHE model. Thus in this work we aimed at developing a tool that could be useful to quantify results of IHC detection of keratinocyte differentiation markers in RHE samples.

3.2. Materials and methods

The reconstructed human epidermis (RHE) samples were generated from spontaneously immortalized epidermal keratinocyte HaCaT line. We employed CRISPR/Cas9-mediated genetic modification system to generate cells that differed in the *HSPA2* gene expression levels. The HSPA2 protein was absent in CRISPR-A2.2 cells (gene knockout). Normal endogenous levels of HSPA2 were present in CRISPR-CTR control cells. RHE samples were generated in vitro according to protocol described in Gogler-Pigłowska 2018 [17]. RHE were fixed in formalin, embedded in paraffin according to standard protocol [17]. The 5 µm thick RHE sections were cut, placed on glass slides, deparaffinized and processed for immunohistochemistry [15]. Endogenous peroxidase activity was blocked for 10 min in 1.5% perhydrol solution. Next, samples were incubated for 45 minutes in 2.5% normal horse serum solution to block endogenous antigens. The ImmPRESS® HRP Universal Antibody (Horse Anti-Mouse/Rabbit IgG) Polymer Detection Kit, Peroxidase, (Vector Laboratories, Burlingame, California, nr MP-7500) was used for detection of antigen-antibody complex according to manufacturer's instruction.

The samples were incubated with the primary anti-K10 antibody (BioLegend, San Diego, California, nr 905401) at 1:3000 dilution at 4°C overnight. DAB chromogen was used to develop IHC staining. Samples were incubated with DAB substrate for 3 minutes at room temperature, and then were counter-stained with hematoxylin for 1 min.

IHC staining was observed using a ZEISS AXIOPHOT light microscope at 200x magnification (10x eyepiece, 20x lens), the images were taken using a Zeiss Axiocam 503 color camera and a ZEN 2.6 photo archiving system.

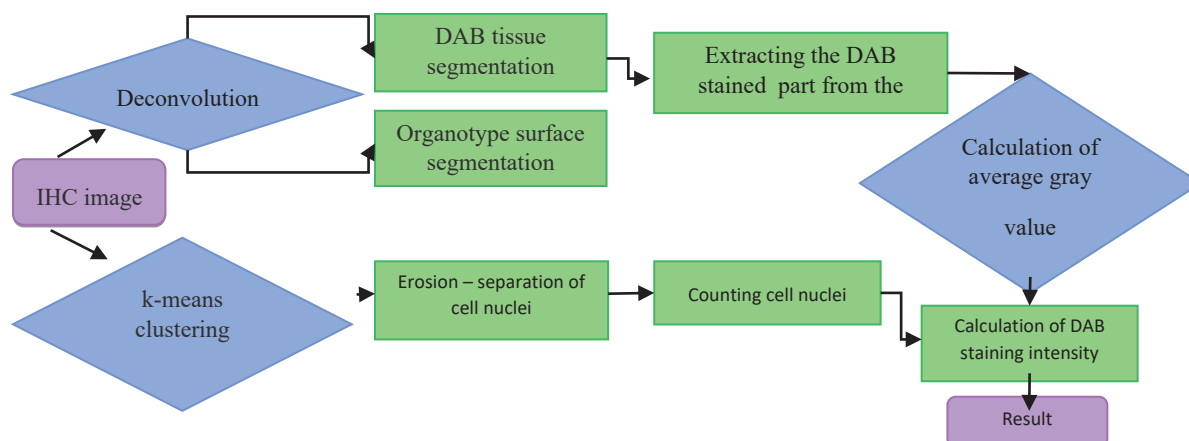


Fig. 1. Flowchart of the IHC quantification program. The program was developed to quantitatively analyze images from IHC staining. Main steps of the algorithm include color image deconvolution of double-stained tissue, calculation the average intensity of pixels in segmented DAB-stained tissue, K-means clustering for nuclei segmentation, counting cell nuclei and calculation the DAB staining intensity normalized by the number of nuclei. The aim of this algorithm is to get quantitative determination of protein expression from IHC images

Rys. 1. Schemat blokowy programu ilościowego IHC. Program został opracowany do ilościowej analizy obrazów z barwienia IHC. Główne etapy algorytmu obejmują dekonwolucję obrazu kolorowego podwójnie zabarwionej tkanki, obliczenie średniej intensywności pikseli w segmentowanej tkance zabarwionej DAB, grupowanie K-średnich dla segmentacji jąder, zliczanie jąder komórkowych i obliczanie intensywności barwienia DAB znormalizowanej przez liczbę jądra. Celem tego algorytmu jest ilościowe określenie ekspresji białek na podstawie obrazów IHC

3.3. Results and discussion

3.3.1. Image Processing

The first step of the algorithm were normalization and deconvolution of images. Image deconvolution is a technique that relies on transformation of color images of multiple-stained tissue (Fig. 2A) into images representing one stain concentration (Fig. 2B, C). The IHC-generated images consisted of three different staining/convolutions: DAB signal, hematoxylin signal and DAB/hematoxylin interference signal. Our aim was to breaking down these tangles without damaging individual signals. Values of parameters P1, P2 and P3 necessary to separate the information contained in the images were taken from the Fiji program for the DAB option (Table 1).

Table 1

Values of parameters obtained from the Fiji program

Signal	P1	P2	P3
Hematoxylin	0.6500286	0.704031	0.2860126
DAB	0.26814753	0.57031375	0.77642715
Residual	0.7110272	0.42318153	0.5615672

The next step was to normalize these values using vector normalization from the group of one signal. Then, a matrix was made of them and used for splitting the signals. Tissue surface was segmented and the average value of pixels intensity was counted. This analysis was conducted using picture in gray scale (Fig. 2).

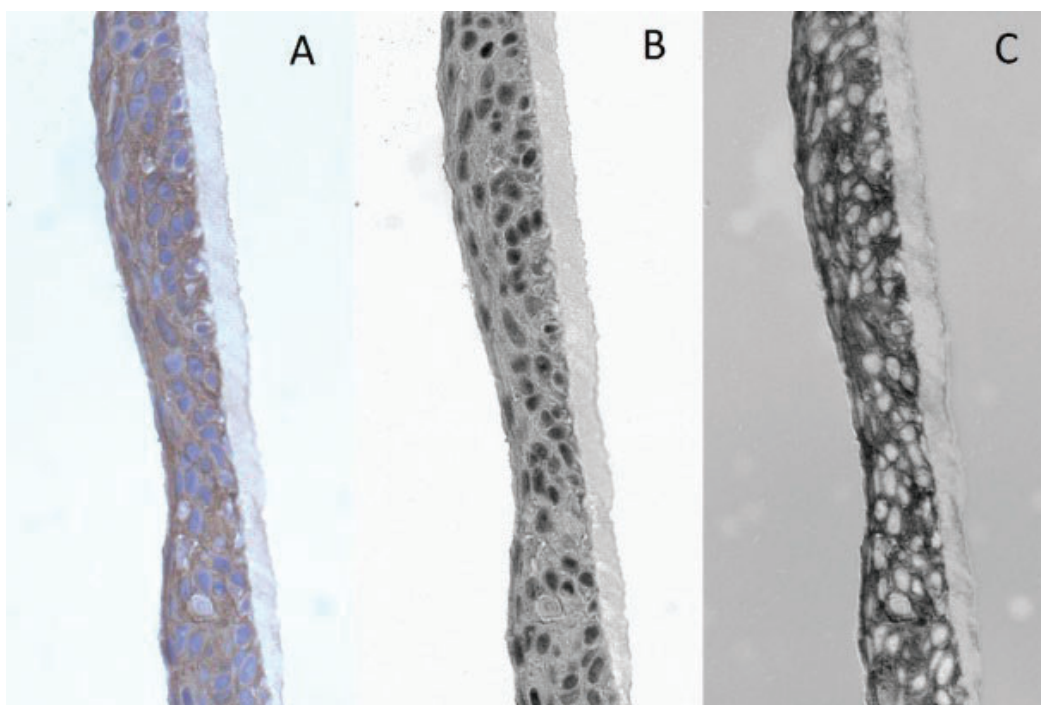


Fig. 2. Deconvolution of IHC image. First step of IHC image processing is deconvolution of signals contained in color IHC image (A). The images obtained after dyeing consisted of three convolutions: DAB signal, hemaotoxylin signal and interference. Implemented program gives individual signals for: nuclei stained with hematoxylin (B) and antigen stained with DAB (C)

Rys. 2. Dekonwolucja obrazu IHC. Pierwszym etapem przetwarzania obrazu IHC jest dekonwolucja sygnałów zawartych w kolorowym obrazie IHC (A). Obrazy otrzymane po barwieniu składały się z trzech splotów: sygnału DAB, sygnału pochodzącego z hematoksyliny i interferencji. Zaimplementowany program daje nam indywidualne sygnały: barwienia hematoksyliną jąder komórkowych (B) i barwienia DAB (C)

The next step was counting average value of pixels intensity in DAB signal area. To get an image of DAB-stained tissue picture containing signal of DAB staining (Fig. 3B) were converted to black and white pixels by image thresholding (Fig. 3A). The next

step was multiplication of original image which represent the DAB signal (Fig. 3B) by the black and white mask (Fig. 3A). As a result we get segmented area of DAB signal in grayscale color (Fig. 3B) and this picture was used to farther analysis.

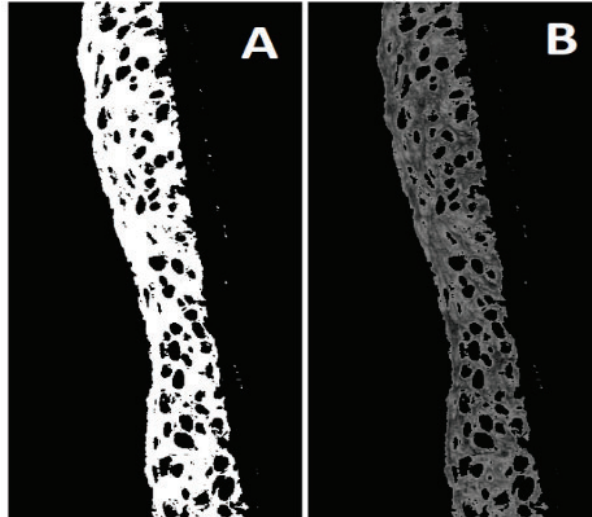


Fig. 3. Segmented area of DAB signal. First to get this result program takes DAB signal and IHC image is converted to black and white pixels by image thresholding (A). Next original image which represent the DAB signal is multiplied by the black and white mask. As a result we get segmented area of DAB signal in grayscale color (B)

Rys. 3. Segmentowany obszar sygnału DAB. Jako pierwszy, aby uzyskać ten wynik, program pobiera sygnał DAB, a obraz IHC jest konwertowany na czarno-białe piksele przez progowanie obrazu (A). Następny oryginalny obraz reprezentujący sygnał DAB jest mnożony przez czarno-białą maskę. W rezultacie otrzymujemy segmentowany obszar sygnału DAB w kolorze skali szarości (B)

Very important part of the image processing workflow was nucleus segmentation and counting. For segmentation purposes k-means clustering was used, which allows to isolate objects by assigning them to one of k groups. The result was an image with 3 colors: black, white and gray. We used three different masks in this step (Fig. 4). Each picture has different clustering result, so the program automatically selects the mask for further analysis.

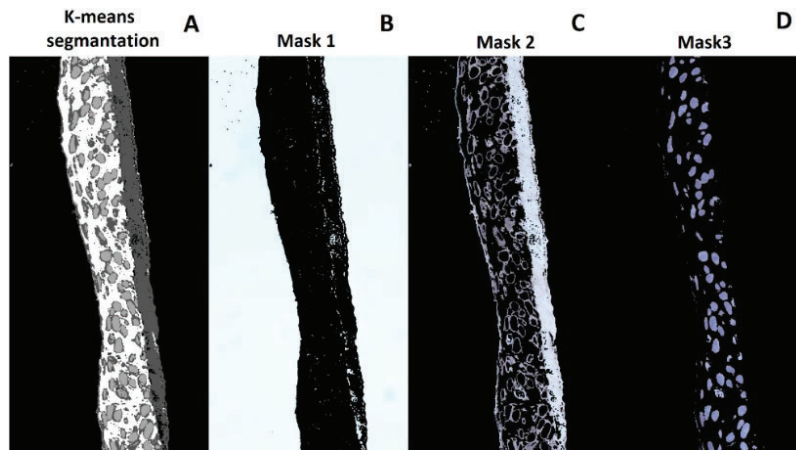


Fig. 4. Results of K-means segmentation and used masks. K-means segmentation was performed using original RGB image. The result was an image with 3 colors: black, white and gray (A). Next we used three different masks (B, C, D). Each picture represent different clustering result. Mask of interest is the one that gives us an image containing blue nuclei (Mask 3). These steps were necessary to allow nucleus counting

Rys. 4. Wyniki segmentacji K-średnich i stosowanych masek. Segmentację K-średnich przeprowadzono przy użyciu oryginalnego obrazu RGB. W rezultacie powstał obraz w 3 kolorach: czarnym, białym i szarym (A). Następnie użyliśmy trzech różnych masek (B, C, D). Każdy obraz przedstawia inny wynik grupowania. Interesująca maska to taka, która daje nam obraz zawierający niebieskie jądra (Maska 3). Te kroki były konieczne, aby umożliwić liczenie jąder

Mask of interest is the one that gives an image containing blue nuclei (Fig. 4D). Next step is getting rid of artifacts. Single pixels also can interfere with the results. The size of the nuclei was irrelevant for analysis, so the solution was the multiple erosion and dilatation of objects (nuclei). The results of the algorithm with the selected nuclei were then visualized (Fig. 5).

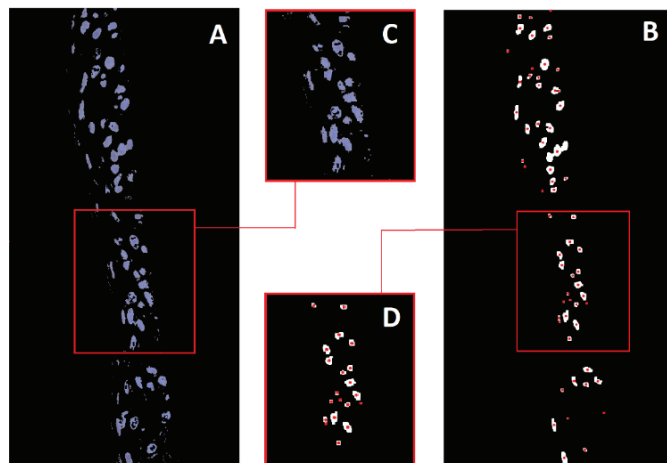


Fig. 5. Selected nuclei. After clustering of image, which we get as result of k-means segmentation, program automatically selected the picture useful for nuclei counting (A). Next image is converted to black and white pixels and each white shape is detected by the algorithm (B). To better visualization enlarged section have also been inserted (C, D)

Rys. 5. Wybrane jądra. Po zgrupowaniu obrazu, które otrzymamy w wyniku segmentacji k-średnich, program automatycznie wybrał obraz przydatny do zliczania jąder (A). Następny obraz jest konwertowany na czarno-białe piksele, a każdy biały kształt jest wykrywany przez algorytm (B). Dla lepszej wizualizacji wstawiono również powiększony przekrój (C, D)

The last step of algorithm is counting intensity of DAB staining normalized by the number of nuclei. Immunohistochemical staining showing the presence of the K10 protein in three-dimensional equivalents of the epidermis obtained from HaCaT cells that differed in levels of the HSPA2 chaperone. The protein was absent in CRISPR-A2.2, while CRISPR-CTRL cells contained normal endogenous levels of HSPA2.

3.3.2. Analysis of DAB-mediated staining of K10 in RHE samples

K10 staining, visible as a brown color, was observed in all examined RHE samples. The results of IHC detection of K10 in RHE corresponded to the typical pattern for K10 immunostaining in the human epidermis. As expected K10, as an early marker of keratinocyte differentiation, was detected in the cytoplasm of keratinocytes located in the suprabasal layers of RHE. However microscopic evaluation of K10-stained samples showed that K10 staining was clearly stronger in RHE generated from CRISPR-A2.2 cells without HSPA2 protein (Fig. 6) than from HSPA2-expressing CRISPR-CTRL cells.

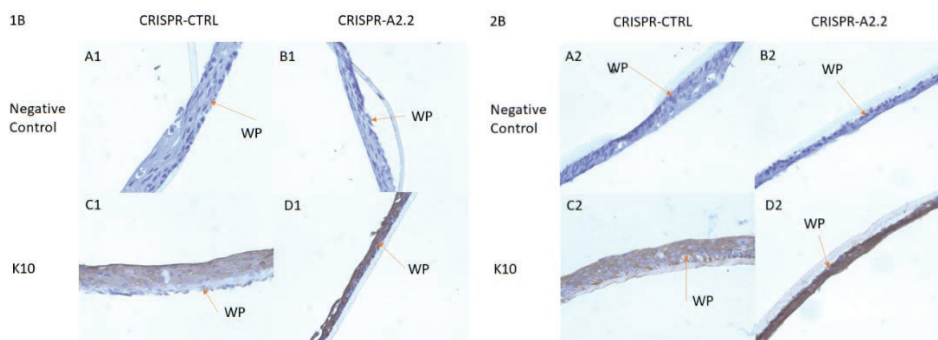


Fig. 6. Immunohistochemical staining showing the presence of K10 protein in RHE obtained from HaCaT cells with varying levels of the HSPA2 chaperone. 1B and 2B are RHE generated in two irrespective biological replicates. Negative control, images without DAB signal (lack of primary antibody) (A1, B1, A2, B2). K10, pictures showing DAB-mediated staining of K10 (C1, D1, C2, D2). CRISPR-CTRL, RHE generated from HSPA2-expressing cells (A1, C1, A2, C2); CRISPR-A2.2, RHE generated from HSPA2-knockout cells (B1, D1, B2, D2). WP- basement membrane. K10 immunoreactivity was clearly stronger in RHE obtained from cells without HSPA2 protein

Ryc. 6. Barwienie immunohistochemiczne wykazujące obecność białka K10 w 3D ekwiwalentach naskórka uzyskanych z komórek HaCaT o różnych poziomach białka opiekuńczego HSPA2. 1B i 2B to powtórzenia użyte w badaniach. WP- warstwa podstawna. Kontrola negatywna oznacza obrazy bez sygnału DAB (brak przeciwciała pierwszorzędowego) (A1, B1, A2, B2). K10 to obrazy z sygnałem DAB w miejscu, w którym występuje keratyna 10 (C1, D1, C2, D2). CRISPR-CTRL pokazuje tkankę z białkiem HSPA2 (A1, C1, A2, C2), a CRISPR-A2.2 pokazuje tkankę bez białka HSPA2 (B1, D1, B2, D2). Barwienie immunohistochemiczne wykazuje różnicę w natężeniu sygnału DAB (odpowiadającego na poziom K10) pomiędzy równoważnikami uzyskanymi z kontrolnych komórek HaCaT (CRISPR-CTRL) a tymi uzyskanymi z komórek z niedoborem białka HSPA2 (CRISPR-A2.2). Immunoreaktywność K10 była wyraźnie silniejsza w organotypach uzyskanych z komórek bez białka HSPA2

Therefore we used the algorithm for quantitative analysis of K10 staining to assess potential differences in K10 expression in quantitative manner. The algorithm for quantitative analysis of DAB-stained RHE was used for two irrespective biological repeats. The 1B repeat group consisted of 11 images taken for RHE generated from CRISPR-CTRL cells and 2 images taken for RHE generated of CRISPR-A2.2 cells. The 2B repeat group consisted of 4 images taken for CRISPR-CTRL and 5 images taken for CRISPR-A2.2 RHE. The mean value for each replicate was calculated. The differences in the intensity of K10 staining between CRISPR-CTRL and CRISPR-A2.2 groups were expressed relative to CRISPR-CTRLs. Results in Fig. 7 show that RHE generated from HSPA2-deficient cells (CRISPR-A2.2) expressed increased level of K10 when compared to RHE generated from CRISPR-CTRL control. This indicates that the lack of HSPA2 protein correlates with increase in K10 expression in RHE.

This results is consistent with our previous findings showing that lowering the level of the HSPA2 protein due to partial suppression of the *HSPA2* gene expression by the RNAi mechanism resulted in a set of keratinocyte phenotypic changes associated with differentiation [17]. The histological and ultrastructural research conducted in parallel with this engineering work have shown that HSPA2-null keratinocytes in comparison to control ones form definitely thinner RHE with residual granular layer (A. Gogler-Piğłowska, work in preparation). Thus, alterations in K10 expression can reflect impaired differentiation of HSPA2-null keratinocytes in RHE model. Therefore, these results confirm that HSPA2 can be an important regulator of keratinocyte differentiation in the epidermis. However, it can be also speculated that higher level of K10 in HSPA2-null RHE can be a direct effect of a total lack of HSPA2 chaperone activity such as abberant K10 folding, altered posstranslational modifications or decreased degradation. This possibilities can be examined in subsequent study.

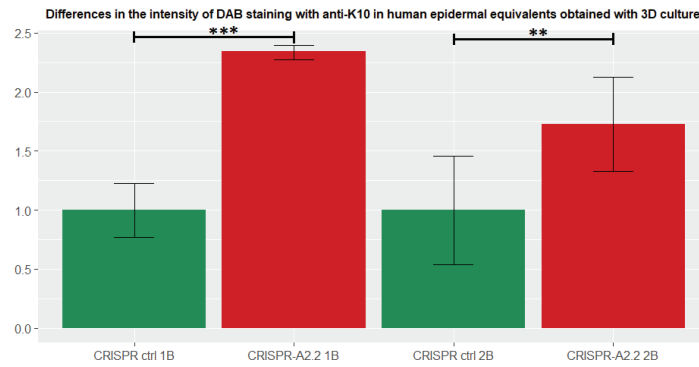


Fig. 7. Differences in the intensity of DAB signal in RHE samples incubated with anti-K10 antibody. The diagram shows results of the program operation for CRISPR-CTRL, with HSPA2 protein CRISPR-A2.2, without HSPA2 protein. Significance was calculated using a one-tailed t-test. For the 1B repeat p-value was 0.00052 and for 2B repeat – 0.0016

Rys. 7. Różnice w intensywności barwienia DAB anty-K10 w ludzkich odpowiednikach naskórka uzyskanych z hodowli 3D. Diagram przedstawia wyniki działania programu dla CRISPR-CTRL, z białkiem HSPA2 i CRISPR-A2.2, bez białka HSPA2. Średnia zmiana w poziomach K10 została obliczona w stosunku do CRISPR-CTRLs, które ustawiono na 1. Jak widzimy, poziomy K10 wzrosły w porównaniu z kontrolą około 2 razy. Istotność obliczono stosując jednostronny test t. Dla powtórzenia 1B p-wartość wyniosła 0.00052, a dla powtórzenia 2B – 0.0016

3.3.3. Evaluation of the possibility of using the algorithm on unstained samples

The program was validated using tissue pictures without DAB staining and without the use of a primary antibody (Fig. 8). When deconvolving pictures without brown DAB response, the signals were split incorrectly. The DAB signal was not visible (the picture is uniformly light gray). This circumstance disturbs the next steps of the algorithm. The aim of the pictures representing DAB staining is to isolate the stained tissue from the image. In a case when DAB signal is absent the program segments the background (Fig. 8 E). It causes an error during calculation of average gray intensity of the area. In the end we obtain very high values of “normalized intensity of DAB staining”, which we can reject basis after inspecting the received images.

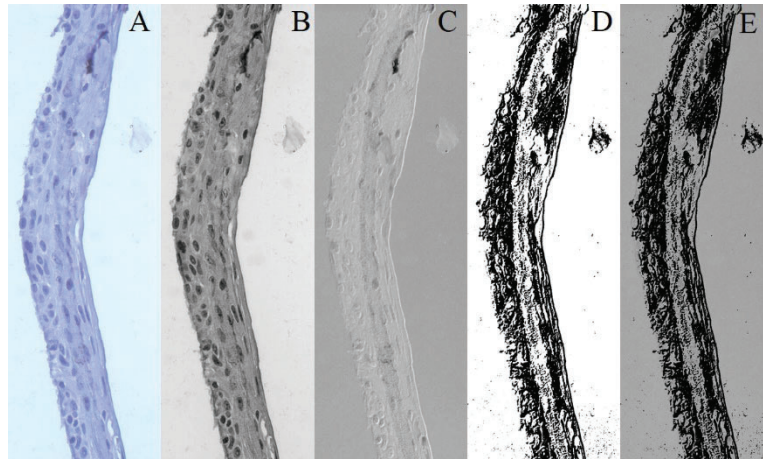


Fig. 8. Results of processing image without DAB signal. The presented images were obtained as a result of the analysis of the image showing no brown color (tissue without primary antibody). We only see purple hematoxylin (A). The C image should show the DAB signal, but it was not present on the specimen, so we cannot see it. This is correct. The presented formulation comes from repeat 1B. Image A shows the original photo. Picture B is the hematoxylin signal, picture C is the DAB signal. In image D we can see image C segmentation and background detail, and in image E grayscale has been superimposed over it

Rys. 8. Wyniki przetwarzania obrazu bez sygnału DAB. Prezentowane obrazy uzyskano w wyniku analizy obrazu nie wykazującego brązowego zabarwienia (preparaty bez użycia przeciwciała pierwszorzędowego). Widzimy tylko fioletową hematoksylinę (A). Obraz C powinien pokazywać sygnał DAB, ale na preparacie go nie było, więc go nie widzimy. Prezentowany preparat pochodzi z powtórzenia 1B. Zdjęcie A przedstawia oryginalne zdjęcie. Obraz B to sygnał hematoksyliny, obraz C to sygnał DAB. Na obrazie D widzimy segmentację obrazu C i szczegóły tła, a na obrazie nałożono na niego skalę szarości

3.4. Summary

The created program allowed for quantitative analysis of DAB-mediated IHC staining in samples of reconstructed human epidermis in vitro that occupy only a small area of the image. In this case the freeware Fiji program with the Immunohistochemistry (IHC) Image Analysis Toolbox- IHC_Toolbox.jar extension showed a poor performance in image analysis. The main limitation was that the whole image (the specimen and background) was analysed by the Fiji program as the test specimen. Thus, Fiji program generated erroneous results when tissues occupying only a fragment of the image surface were analyzed. Our program allows to overcome this limitation and provided the tool to calculate DAB staining intensity in tissues that do not cover the entire surface of the image taken. Also, our program accelerates the analysis of the long and narrow specimens (such as the epidermis) that cover only a part of image because it eliminates a need for cutting the specimen-covered area off

the each individual photograph. This initial and time-consuming step in image analysis pipeline with Fiji program is hard to accept when a large set of DAB-stained specimens need to be analysed.

Acknowledgement

Many thanks to Professor Dorota Ścieglińska and her team consisting of Dr. Agnieszka Gogler-Pigłowska, Dr. Damian Sojka, MSc Małgorzata Adamiec-Organiściok, who made it possible to perform the scientific research, and also to Professor Magdalena Skonieczna, thanks to whom I learned many laboratory techniques. Many thanks to Dr. Roman Jaksik, who allowed me to discover our potential and helped us write the article.

This work was supported by the National Science Centre, Poland, under research grant project No. 2017/25/B/NZ4/01550 to Dorota Ścieglińska.

Students' Scientific Society of Biotechnology was supported in the 8th edition of funding for student research in Project Based Learning under the Excellence Initiative – Research University program, in accordance with Rector's of the Silesian University of Technology Regulation No. 54/2020 and 55/2020 issued March 13, 2020.

Bibliography

1. T. Wolski, B. Kędzia: Farmakoterapia skóry. Cz. 1. Budowa i fizjologia skóry. *Postępy Fitoterapii* 1/2019, 2019, s. 61–67.
2. I. Colombo, E. Sangiovanni, R. Maggio, C. Mattozzi, S. Zava, Y. Corbett, M. Fumagalli, C. Carlino, P.A. Corsetto, D. Scaccabarozzi, S. Calvieri, A. Gismondi, D. Taramelli, M. Dell'Agli: HaCaT Cells as a Reliable In Vitro Differentiation Model to Dissect the Inflammatory/Repair Response of Human Keratinocytes. *Mediators of inflammation*, 2017 (2017): 7435621, 2017.
3. R.B. Presland, B.A. Dale: Epithelial structural proteins of the skin and oral cavity: function in health and disease. *Critical reviews in oral biology and medicine* : an official publication of the American Association of Oral Biologists, 11(4), 383–408, 2000.
4. W. Sawicki: *Histologia dla studentów medycyny. Podręcznik*. Wydawnictwo Lekarskie PZWL, Warszawa 1997.
5. M.B. Murphrey, J.H. Miao, P.M. Zito: *Histology, Stratum Corneum*. StatPearls. 2021.

6. V. Kapuśniak: Proces rogowacenia komórek naskórka, *Medycyna Weterynaryjna*, 62 (1), 2006.
7. S. Eun Lee, S. Hun Lee: Skin Barrier and Calcium. *Ann Dermatol*, 30(3):265–275, 2018.
8. J. Reichelt, C. Bauer, R.M. Porter, E.B. Lane, V. Herzog: Out of balance: consequences of a partial keratin 10 knockout. *Journal of Cell Science* 110, 2175–2186, 1997.
9. S.H. Yuspa, A.E. Kilkenny, P.M. Steinert, D.R. Roop: Expression of Murine Epidermal Differentiation Markers Is Tightly Regulated by Restricted Extracellular Calcium Concentrations In Vitro. *The Journal of Cell Biology*(3):1207–17, 1989.
10. D.D. Bikle, Z. Xie, C. Tu: Calcium regulation of keratinocyte differentiation. *Expert Rev Endocrinol Metab*, 7(4):461–472, 2012.
11. A.S. Évora, M.J. Adams, S.A. Johnson, Z. Zhang: Corneocytes: Relationship between Structural and Biomechanical Properties. *Skin Pharmacol Physiol*, 34:146–161, 2021.
12. <https://wylecz.to/badania-laboratoryjne/badanie-immunohistochemiczne/>, [dostęp: 17.04.2022].
13. V. Dubowitz, C.A. Sewry, A. Oldfors, R. Lane, *MUSCLE BIOPSY*, S. Elsevier, U. Kämmerer, M. Kapp, A.M. Gassel, T. Richter, C. Tank, J. Dietl, P. Ruck: A new rapid immunohistochemical staining technique using the EnVision antibody complex. *The journal of histochemistry and cytochemistry: official journal of the Histochemistry Society*, 49(5), 623–630, 2001.
14. S. Magaki, S. A. Hojat, B. Wei, A. So, W. H. Yong: An Introduction to the Performance of Immunohistochemistry. *Biobanking. Methods in Molecular Biology*, vol 1897. Humana Press, New York 2019.
15. D. Scieglinska, Z. Krawczyk: Expression, function, and regulation of the testis-enriched heat shock HSPA2 gene in rodents and humans. *Cell Stress Chaperones*. 2015;20(2):221–35, doi: 10.1007/s12192-014-0548-X.
16. D. Scieglinska, W. Piglowski, M. Chekan, A. Mazurek, Z. Krawczyk: Differential expression of HSPA1 and HSPA2 proteins in human tissues; tissue microarray-based immunohistochemical study. *Histochem Cell Biol*. 2011;135(4):337–50, doi: 10.1007/s00418-011-0791-5.

- 17.A. Gogler-Pigłowska, K. Klarzyńska, D.R. Sojka, A. Habryka, M. Głowala-Kosińska, M. Herok, M. Kryj, M. Halczok, Z. Krawczyk, D. Ścieglińska: Novel role for the testis-enriched HSPA2 protein in regulating epidermal keratinocyte differentiation. *Journal of Cellular Physiology*, 2017.

A TOOL FOR QUANTIFYING THE LEVEL OF ANTIGEN (KERATIN 10) DETERMINED BY THE IHC METHOD IN HUMAN EPIDERMAL EQUIVALENTS OBTAINED IN VITRO

Abstract

Semi-quantitative IHC is a powerful method that allows to assess protein levels and localization in preserved tissues. This is possible through sophisticated image processing algorithms, which provide the means to quantify the differences in the level of stained protein using deconvolution. Fiji software is an example of such system, however its applications are significantly limited by the requirement to process only those images which are fully filled with the analyzed tissue. When the stained tissue is only part of the image, which is typical in studies of human epidermis, the results are distorted.

The aim of this study was to develop a novel image processing methodology which allows to conduct semi-quantitative analysis of protein levels, based on images which are not completely filled with the stained tissue, and use it to investigate how HSPA2 protein deficiency affects the localization of keratin 10 in human epidermal cells.

Using our automated image processing algorithm we were able to determine, the localization of keratin 10 in organotypic cell cultures. We were also able to assess, the differences in the intensity of keratin 10 staining in the in vitro grown epidermal sections, which allowed us to assess its association with the presence of the HSPA2 protein. The semi-quantitative protein analysis which we propose may contribute to a more detailed understanding of the role of HSPA2 protein in the process of keratinocyte differentiation in human epidermis.

Keywords: Keratin 10, immunohistochemistry, DAB, keratinocytes organotypic culture, HSPA2